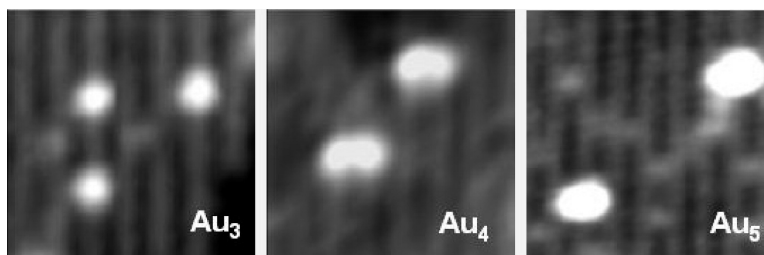


## Intact Size-Selected Au Clusters on a TiO(110)-(1 × 1) Surface at Room Temperature

Xiao Tong, Lauren Benz, Paul Kemper, Horia Metiu, Michael T. Bowers, and Steven K. Buratto

*J. Am. Chem. Soc.*, **2005**, 127 (39), 13516-13518 • DOI: 10.1021/ja052778w • Publication Date (Web): 08 September 2005

Downloaded from <http://pubs.acs.org> on March 25, 2009



### More About This Article

Additional resources and features associated with this article are available within the HTML version:

- Supporting Information
- Links to the 20 articles that cite this article, as of the time of this article download
- Access to high resolution figures
- Links to articles and content related to this article
- Copyright permission to reproduce figures and/or text from this article

[View the Full Text HTML](#)

## Intact Size-Selected Au<sub>n</sub> Clusters on a TiO<sub>2</sub>(110)-(1 × 1) Surface at Room Temperature

Xiao Tong, Lauren Benz, Paul Kemper, Horia Metiu, Michael T. Bowers, and Steven K. Buratto\*

*Department of Chemistry and Biochemistry, University of California, Santa Barbara, California 93106*

Received June 3, 2005; E-mail: buratto@chem.ucsb.edu

Nanoparticle size is an important parameter affecting the catalytic behavior of nanostructured metal/oxide catalysts.<sup>1–5</sup> Heiz et al. showed that the catalytic activity of Au<sub>n</sub> ( $n \leq 20$ ) on MgO (100) films in the oxidation of CO was highest for Au<sub>18</sub> and that Au<sub>8</sub> was the smallest cluster which exhibited catalytic behavior.<sup>3</sup> A similar investigation at room temperature involving Au<sub>n</sub> ( $n = 1–4, 7$ ) supported on rutile TiO<sub>2</sub>(110) by Anderson et al. suggests a strong size dependence in the oxidation of CO, with significant reactivity for clusters as small as Au<sub>3</sub>.<sup>4</sup> While these two studies show a strong dependence of the catalytic activity on the deposited cluster size, the eventual size (and shape) of the metal clusters once they were deposited on the substrate was not measured directly in either case. It is well-known from scanning tunneling microscopy (STM) images of evaporated Au and Ag, assumed to be monomeric in the vapor phase, that these metals sinter upon reaching the surface of TiO<sub>2</sub> to form larger clusters ( $\gg 10$  atoms).<sup>6–10</sup> Additionally, the size distribution of clusters formed by depositing size-selected metal clusters on a substrate is often not well defined due to cluster diffusion and aggregation at low landing energies (a few eV/atom) or fragmentation and implantation at higher landing energies ( $\sim 100$  eV/atom), respectively.<sup>11,12</sup> Thus, determining whether the mass-selected clusters deposited softly on a surface maintain their size after deposition is an important goal of research on catalysis by nanoclusters.<sup>13</sup> In the experiments described here, we use ultrahigh vacuum (UHV) STM to image the shape and size of the Au<sub>n</sub><sup>+</sup> clusters ( $n = 1–8$ ) deposited with low kinetic energy on a single crystal rutile TiO<sub>2</sub>(110)-(1 × 1) surface at room temperature. The atomic resolution STM images allow us to directly identify the shapes, adsorption sites, and size distributions of the adsorbed clusters.

The size-selected clusters of Au<sub>n</sub><sup>+</sup> ( $n = 1–8$ ) are created using laser desorption from a gold rod illuminated with a pulsed YAG laser beam (532 nm, 500 mJ/pulse max power), producing a gold plasma. Positive ion clusters are extracted and accelerated through a skimmer in an argon carrier gas. The clusters are then focused, further accelerated, and passed between the pole faces of a magnet, where the size-selection process occurs. The mass resolution is  $\sim 10\%$ . The size-selected cluster ion beam, which has a flux of  $\sim 1$  nA/cm<sup>2</sup>, is focused on a positively biased TiO<sub>2</sub>(110)-(1 × 1) sample in a UHV chamber with a base pressure of less than  $1 \times 10^{-9}$  Torr during deposition. The sample bias is set to lower the incident kinetic energy of the clusters to less than 2.0 eV/atom, resulting in soft-landing conditions. Exposure times of 20–60 min at room temperature (RT) result in a surface coverage of  $\sim 0.02–0.06$  ML for all the samples. Prior to cluster deposition, the clean TiO<sub>2</sub>(110)-(1 × 1) surface was prepared by multiple cycles of Ar<sup>+</sup> ion sputtering of the crystal (1 keV, 20 min), followed by flashing at  $\sim 850$  °C. Empty state STM images of the surface were acquired at RT, in constant current mode, with a sample bias of +1 to +2 V and a tunneling current of 0.1–0.2 nA on an RHK SPM 100 in a chamber with base pressure of less than  $2 \times 10^{-10}$  Torr.

Figure 1A shows large clusters on the surface resulting from the deposition of Au<sub>1</sub><sup>+</sup>. A magnified region of this image, shown in Figure 1a, reveals that there are no small clusters on surface. These observations indicate that Au monomers are highly mobile on the rutile surface, leading to aggregation into larger clusters. Figure 2a shows a broad height distribution for the deposition of Au atoms with an average value of 4.3 Å (Figure 3) and a standard deviation of 1.7 Å. This result is similar to that observed from Au vapor deposition in the coverage region of 0.013–0.08 ML.<sup>18</sup> These sintered clusters have an average lateral diameter of  $14.8 \pm 3.9$  Å, which indicates that an average cluster contains on the order of tens of atoms.

Figure 1B shows an STM image taken after the deposition of Au<sub>2</sub><sup>+</sup>. In contrast to the monomer deposition, large, sintered clusters are rarely observed. Instead, a high density of very small clusters is seen, and most of them are located above the 5-fold coordinated titanium (5c-Ti) rows (Figure 1b). The height distribution is much narrower than that found in the case of the Au<sub>1</sub> deposition, as shown in Figure 2b. The clusters on the surface have an average height of 1.6 Å (Figure 3) and a standard deviation of 0.5 Å, suggesting that the adsorbed Au<sub>2</sub> clusters lay flat on the surface. The nearly uniform height and the preference for certain adsorption sites suggest that the adsorbed Au<sub>2</sub> clusters remain intact during landing.

Only small clusters are observed for Au<sub>3</sub><sup>+</sup> (Figure 1C), and they are found mainly above the 5c-Ti rows (Figure 1c). The height distribution is narrow (Figure 2c) with an average value of 1.5 Å (Figure 3) and a standard deviation of 0.2 Å. As in the case of dimer deposition, this suggests that the adsorbed Au<sub>3</sub> are intact and that the clusters lay flat on the surface.

Small clusters were also observed after the deposition of Au<sub>4</sub><sup>+</sup> (see Figure 1D and 1d). The height distribution for Au<sub>4</sub> clusters is shown in Figure 2d with an average height of 1.7 Å (Figure 3) and a standard deviation of 0.2 Å, suggesting that adsorbed Au<sub>4</sub> lays flat on the surface. The shape distribution of the Au<sub>4</sub> clusters on the surface is also interesting. The dominant shape is the two-lobe structure shown in Figure 1d. The center of the two lobes is always observed on a bridging O row. The average distance between the two lobes is about 7 Å (given the 5c-Ti row spacing of 6.5 Å, suggesting a quasi-linear structure, possibly with an elongated central Au–Au bond). The unique shape and sharp size distribution (Figure 2d) resulting from the deposition of Au<sub>4</sub> suggest the clusters remain intact on the surface.

Figure 1E shows small clusters resulting from the deposition of Au<sub>5</sub><sup>+</sup>. Most features are located over the 5c-Ti rows, as shown in Figure 1e. The height distribution is narrower than that of Au<sub>1</sub>, but wider than that of Au<sub>2</sub>, Au<sub>3</sub>, and Au<sub>4</sub> (Figure 2e). The clusters have an average height of  $2.6 \pm 0.6$  Å (Figure 3), suggesting that adsorbed Au<sub>5</sub>, unlike Au<sub>2</sub>, Au<sub>3</sub>, and Au<sub>4</sub>, is either strongly buckled or consists of two atomic layers.

Figure 1F and 1f shows features resulting from the deposition of Au<sub>6</sub><sup>+</sup> clusters. Most features are located over the 5c-Ti rows.

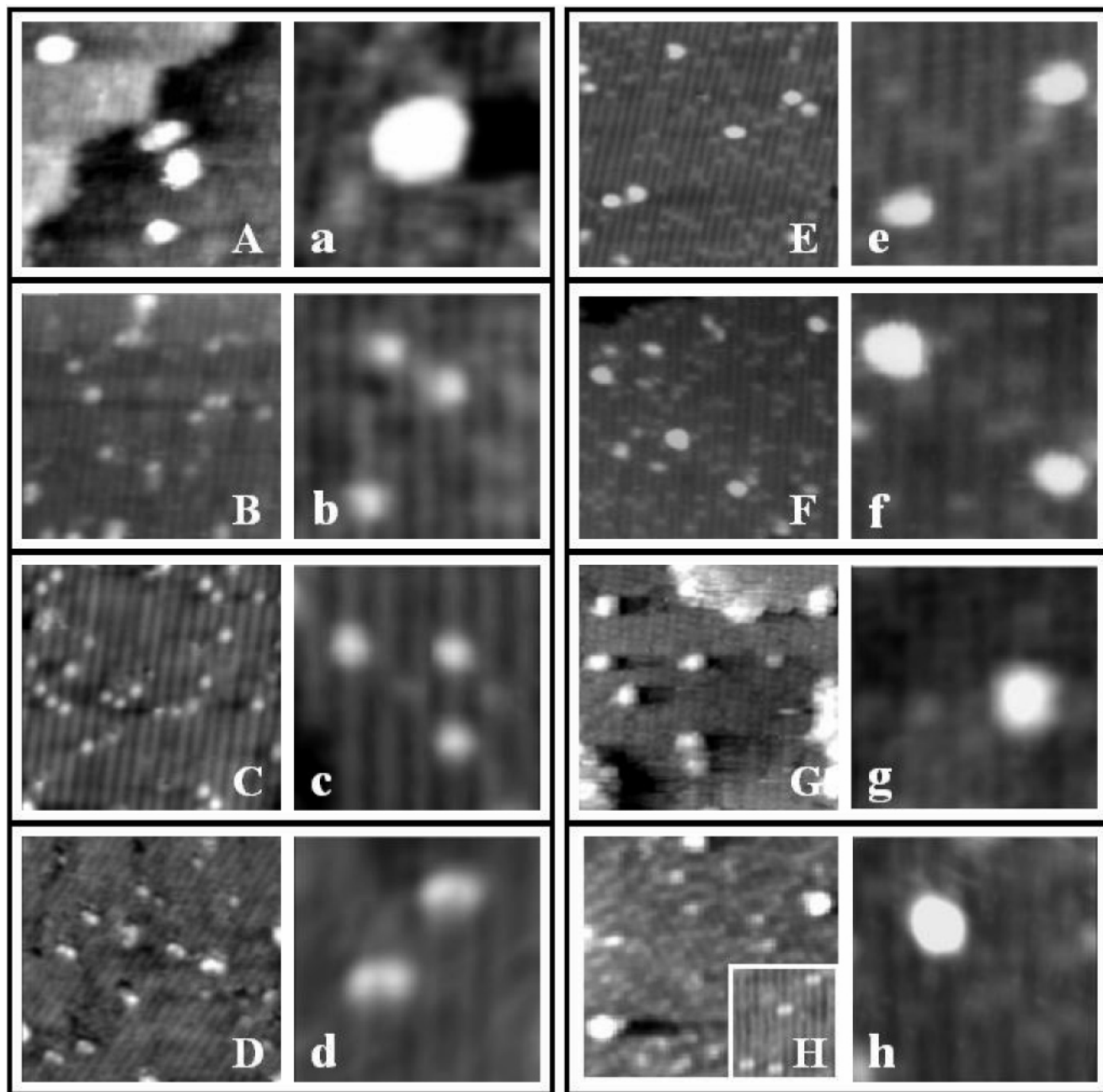


**Figure 1.** STM images  $140 \text{ \AA} \times 140 \text{ \AA}$  (uppercase letters) and  $50 \text{ \AA} \times 50 \text{ \AA}$  (lowercase letters) of the same surfaces, respectively. The bright spots are the clusters. The bright stripes are the 5-fold coordinated Ti atom (5c-Ti) rows separated by  $6.5 \text{ \AA}$  by the bridging oxygen rows, which are dark.<sup>14</sup> The dim spots that appear on the bridging oxygen rows are bridging oxygen vacancies.<sup>10,15–17</sup> (A/a) The  $\text{TiO}_2$  surface after the deposition of  $\text{Au}_1$ . (B/b) The same for  $\text{Au}_2$ . (C/c) The same for  $\text{Au}_3$ . (D/d) The same for  $\text{Au}_4$ . (E/e) The same for  $\text{Au}_5$ . (F/f) The same for  $\text{Au}_6$ . (G/g) The same for  $\text{Au}_7$ . (H/h) The same for  $\text{Au}_8$ . The scale of the inset in H is  $65 \text{ \AA} \times 75 \text{ \AA}$ .

Their size distribution (Figure 2f) has an average height of  $2.3 \pm 0.7 \text{ \AA}$  (Figure 3) and is similar to that of  $\text{Au}_5$ , suggesting a buckled or a bilayer structure on the surface.

The result from the deposition of  $\text{Au}_7^+$  is shown in Figure 1G and 1g. The height distribution (Figure 2g) shows an average height of  $2.8 \pm 0.7 \text{ \AA}$  (Figure 3) for these clusters, which is similar to that obtained for both  $\text{Au}_5$  and  $\text{Au}_6$ . This suggests that the  $\text{Au}_7$  clusters adopt a three-dimensional structure on surface. Most of the  $\text{Au}_7$  clusters are located above the bridging oxygen rows (Figure 1g), which is different from both the  $\text{Au}_5$  and  $\text{Au}_6$  clusters. The unique adsorption site and slightly different height suggest the presence of intact  $\text{Au}_7$  clusters on the surface.

Figures 1H and 1h show features resulting from deposition of  $\text{Au}_8^+$  clusters. The height distribution (Figure 2h) gives an average

height of  $2.7 \pm 0.9 \text{ \AA}$  (Figure 3) for these clusters. This suggests that the  $\text{Au}_8$  clusters also adopt a three-dimensional structure on the surface with a similar average height as  $\text{Au}_5$ ,  $\text{Au}_6$ , and  $\text{Au}_7$ . The high-resolution STM image of  $\text{Au}_8$  in the inset of Figure 1H shows that a small percentage (<5% of clusters) of the deposited  $\text{Au}_8$  clusters dissociate to pairs of the two-lobed  $\text{Au}_4$  species, which appear particularly stable on the  $\text{TiO}_2(110)$  surface. No other cluster dissociations are observed for the systems reported here.

The results presented here are consistent with a number of earlier studies and provide some new, unexpected and important information. Soft-landing gold atoms lead to rapid sintering and formation of globules with an average height consistent with four atomic layers. Earlier STM studies on titania with larger coverages from evaporative gold sources indicated significant sintering and forma-

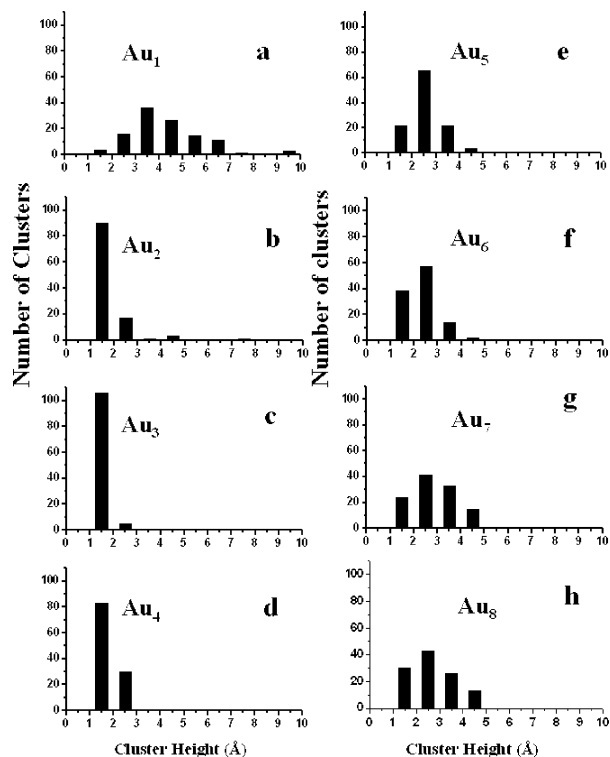


**Figure 2.** The cluster height distributions of deposited  $Au_n$  ( $n = 1-8$ ) on  $TiO_2(110)-(1 \times 1)$  surface.

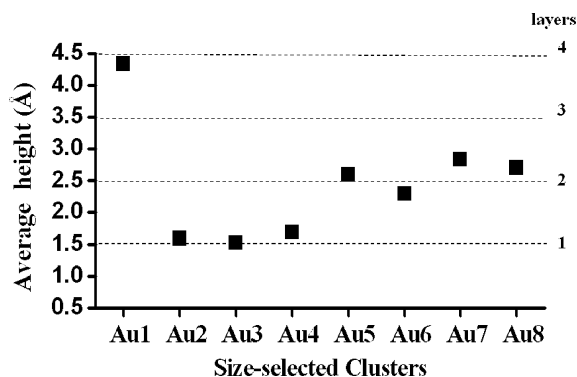


**Figure 3.** The average cluster heights of  $Au_n$  ( $n = 1-8$ ) on the  $TiO_2(110)-(1 \times 1)$  surface. The dashed lines indicate heights expected for various gold layers in the cluster.

tion of very large globules. Our low coverage, single atom depositions thus confirm the high mobility of Au atoms on titania and their tendency to sinter.

A surprise for us is the fact that clusters as small as the Au dimer have very limited mobility and do not sinter. By contrast, soft-landed silver dimers do sinter,<sup>19</sup> forming globules of approximately the same size as the gold atom results presented here. Most likely, these results reflect the binding energies of silver and gold clusters to the surface of titania, which is a topic we will address in a future publication.

Gold dimers, trimers, and tetramers all lie flat on the surface, while  $Au_5$ ,  $Au_6$ ,  $Au_7$ , and  $Au_8$  all exhibit two-layer, three-dimensional structures. This is a surprising observation given that both theory and experiment indicate that isolated cationic gold clusters<sup>20</sup> are planar at least to  $Au_7^+$  and that anionic gold clusters<sup>21</sup> are planar to at least  $Au_{12}^-$ . The data in Figure 3 clearly indicate that the 2-d to 3-d transition occurs at  $n = 5$  for neutral gold clusters on titania. Thus, the larger gold clusters bound to the surface adopt a different structure than in the gas phase.

The surface can have two effects on the gold cluster. First, electron transfer can occur from the surface to the cluster. This effect would favor planar structures based on gas-phase results.<sup>20,21</sup> Second, the surface can specifically ligate the cluster. The primary ligation sites are the bridging oxygen atoms, separated by 6.5 Å between rows. The tetramer is the smallest cluster able to span across two adjacent rows and then only if a quasi-linear structure is invoked, a structure consistent with the two-lobed image we observe for  $Au_4$ . This result suggests that surface ligation is driving cluster structure since the linear form of  $Au_4$  is not favored by theory.<sup>20</sup> Recent results on both silver<sup>22</sup> and gold<sup>23</sup> cluster cations indicate that gas-phase ligation can induce structural change consistent with this observation. The fact that the 2-d to 3-d transition occurs at  $Au_5$  may reflect that the fifth gold atom is not needed for maximal ligation and begins to form a second layer in the cluster. The addition of the sixth and seventh gold atoms to the cluster continues the trend.

The importance of cluster–surface ligation is supported by the fact that the STM images observed were stable over several days and did not change with repeated scans by the STM tip. In addition, we observe a density of oxygen vacancies between clusters for all sizes studied here (see the high-resolution images in Figure 1a–1h). Generally, the density of oxygen vacancies is much higher than what would be expected if each cluster were bound to one or more oxygen vacancies. There is no direct evidence that these defects are required for binding the clusters. In fact, the lack of mobility of clusters as small as the dimer indicates that strong binding occurs with the stoichiometric surface.

**Acknowledgment.** This work was funded by a Defense University Research in Nanotechnology (DURINT) grant (F49620-01-04J9) from the Air Force Office of Scientific Research (AFOSR).

## References

- (1) Haruta, M. *Catal. Today* **1997**, *36*, 153.
- (2) Valden, M.; Lai, X.; Goodman, D. W. *Science* **1998**, *281*, 1647.
- (3) Sanchez, A.; Abbet, S.; Heiz, U.; Schneider, W. D.; Hakkinen, H.; Barnett, R. N.; Landman, U. *J. Phys. Chem. A* **1999**, *103*, 9573.
- (4) Lee, S.; Fan, C.; Tainpin, W.; Anderson, S. L. *J. Am. Chem. Soc.* **2004**, *126*, 5682.
- (5) Yoon, B.; Hakkinen, H.; Landman, U.; Worz, A. S.; Antonietti, J. M.; Abbet, S.; Judai, K.; Heiz, U. *Science* **2005**, *307*, 403.
- (6) Lai, X.; St Clair, T. P.; Valden, M.; Goodman, D. W. *Prog. Surf. Sci.* **1998**, *59*, 25.
- (7) Lai, X. F.; Goodman, D. W. *J. Mol. Catal. A-Chem.* **2000**, *162*, 33.
- (8) Parker, S. C.; Grant, A. W.; Bondzie, V. A.; Campbell, C. T. *Surf. Sci.* **1999**, *441*, 10.
- (9) Wahlstrom, E.; Lopez, N.; Schaub, R.; Thosttrup, P.; Ronnau, A.; Africh, C.; Laegsgaard, E.; Norskov, J. K.; Besenbacher, F. *Phys. Rev. Lett.* **2003**, *90*, 026101.
- (10) Tong, X.; Benz, L.; Kolmakov, A.; Chretien, S.; Metiu, H.; Buratto, S. K. *Surf. Sci.* **2005**, *575*, 60.
- (11) Bromann, K.; Felix, C.; Brune, H.; Harbich, W.; Monot, R.; Buttet, J.; Kern, K. *Science* **1996**, *274*, 956.
- (12) Bromann, K.; Brune, H.; Felix, C.; Harbich, W.; Monot, R.; Buttet, J.; Kern, K. *Surf. Sci.* **1997**, *377*, 1051.
- (13) Schaub, R.; Jodicke, H.; Brunet, F.; Monot, R.; Buttet, J.; Harbich, W. *Phys. Rev. Lett.* **2001**, *86*, 3590.
- (14) Diebold, U. *Surf. Sci. Rep.* **2003**, *48*, 53.
- (15) Diebold, U.; Lehman, J.; Mahmoud, T.; Kuhn, M.; Leonardelli, G.; Hebenstreit, W.; Schmid, M.; Varga, P. *Surf. Sci.* **1998**, *411*, 137.
- (16) Suzuki, S.; Fukui, K.; Onishi, H.; Iwasawa, Y. *Phys. Rev. Lett.* **2000**, *84*, 2156.
- (17) Schaub, R.; Thosttrup, R.; Lopez, N.; Laegsgaard, E.; Stensgaard, I.; Norskov, J. K.; Besenbacher, F. *Phys. Rev. Lett.* **2001**, *87*, 6104.
- (18) Spiridis, N.; Haber, J.; Korecki, J. *Vacuum* **2001**, *63*, 99.
- (19) Benz, L.; Tong, X.; Kemper, P.; Lilach, Y.; Kolmakov, A.; Metiu, H.; Bowers, M. T.; Buratto, S. K. *J. Chem. Phys.* **2005**, *122*, 081102.
- (20) Gilb, S.; Weis, P.; Furche, F.; Ahlrichs, R.; Kappes, M. M. *J. Chem. Phys.* **2002**, *116*, 4094.
- (21) Furche, F.; Ahlrichs, R.; Weis, P.; Jacob, C.; Gilb, S.; Bierweiler, T.; Kappes, M. M. *J. Chem. Phys.* **2002**, *117*, 6982.
- (22) Manard, M.; Kemper, P.; Bowers, M. T. *J. Am. Chem. Soc.* **2005**, *127*, 9994.
- (23) Kemper, P.; Manard, M.; Bowers, M. T. Manuscript in preparation.

JA052778W